Malaysian Journal of Mathematical Sciences 15(3): 387–396 (2021)

Malaysian Journal of Mathematical Sciences

Journal homepage: https://einspem.upm.edu.my/journal

Hypersingular Integral Equation for Triple Circular Arc Cracks in an Elastic Half-Plane

Husin, N. H.[1], Nik Long, N. M. A.[1,2,*], and Senu, N.[1,2]

[1]*Institute for Mathematical Research, Universiti Putra Malaysia, Malaysia*
[2]*Department of Mathematics & Statistics, Faculty of Science, Universiti Putra Malaysia, Malaysia*

E-mail: nmasri@upm.edu.my
[*]*Corresponding author*

Received: 30 March 2020
Accepted: 19 June 2021

Abstract

Triple circular arc cracks problems subjected to shear stress in half-plane elasticity is investigated. Modified complex potentials (MCP) with the free traction boundary condition are applied to formulate the hypersingular integral equation (HSIE) for the problems. The unknown crack opening displacements (COD) of the HSIE are solved numerically by using the appropriate quadrature formulas. Mode I and Mode II of nondimensional stress intensity factor (SIF) at all cracks tips are presented for the problems of three adjacent circular arc cracks, three circular arc cracks with dissimilar radius and three circular arc cracks in series in a half-plane. The results exhibit that as the crack opening angle increases and the distance of cracks closer to the boundary of half-plane, the nondimensional SIF increases. This indicates that the strength of material becomes weaker and the tendency of material to fail is higher.

Keywords: half-plane; hypersingular integral equation; stress intensity factor; triple circular arc cracks.

1 Introduction

Structural failure may occur for many reasons, including defects in the materials, loading uncertainties, and natural disasters. Presence of cracks is one of the causes that might lead to material failure as it may weaken the strength of materials. Many researchers have proposed various methods to formulate the cracks problems in a half-plane, infinite plane, or bonded dissimilar materials.

Weakly singular integral equation by [3], hypersingular integral equation by [4] and singular integral equation by [7] were applied to formulate curved cracks problems in a half-plane elasticity. Potential theory was proposed for the contact problems and crack in half-plane of transversely isotropic piezoelectric materials by [10]. A distributed dipole technique is used by [9] to analyse the problem for multiple cracks of branced, kinked and straight cracks in a half-plane. [14] calculated the stress intensity factor for cracks in an orthotropic half-plane using the dislocation technique associated with the Cauchy singularity and Fourier transform in the complex form. [15] developed the analysis of cracks problems under mixed-mode condition in an orthotropic half-plane. The cracks problems in a half-plane for more complicated crack configurations were considered by [8].

Recently, the problems of triple cracks have drawn the attention of numerous researchers. The stress intensity factors for the three cracks problem of Griffith cracks on the surface of a pair of nonidentical infinite elastic half-spaces was analysed by [6]. Meanwhile, the stress magnification factors of three coplanar Griffith cracks in a sandwiched of two identical orthotropic half planes was calculated by [5]. [18] formulated the three collinear and parallel circular arc cracks problems using boundary element analysis. [12] applied the Schmidt method for the three cracks at the interface of a graded layer bonding two different materials. Three equal collinear cracks in an orthotropic solid and a homogeneous elastic were considered by [17]. [13] studied the dynamic stress intensity factors in an orthotropic plate subjected to time-harmonic disturbance for the case of three collinear cracks. [1] investigated the three cracks of collinear unequal smooth cracks of an isotropic infinite plate with coalesced yield zones by using the modification of Dugdale model.

In this paper, the problems of triple circular arc cracks in a half-plane elasticity is formulated into HSIE using the MCP and traction free boundary condition. The cracks are mapped into the real axis and are solved numerically. Mode I and Mode II of nondimensional SIFs are discussed and analysed graphically.

2 Mathematical Formulation

The complex potentials of the crack problem is formulated by utilising the complex variable function method. The stresses $(\sigma_x, \sigma_y, \sigma_{xy})$, the resultant force functions (X, Y) and the displacements (u, v) can be demonstrated by the two complex potentials $\Phi(\xi) = \phi'(\xi)$ and $\Psi(\xi) = \psi'(\xi)$ as follows [16]

$$\sigma_x + \sigma_y = 4Re\Phi(\xi), \tag{1}$$

$$\sigma_y + i\sigma_{xy} = 2Re\Phi(\xi) + \xi\overline{\Phi'(\xi)} + \overline{\Psi(\xi)}, \tag{2}$$

$$f = -Y + iX = \phi(\xi) + \xi\overline{\phi'(\xi)} + \overline{\psi(\xi)}, \tag{3}$$

$$2G(u + iv) = \kappa\phi(\xi) - \xi\overline{\phi'(\xi)} - \overline{\psi(\xi)}, \tag{4}$$

where $\xi = \xi_x + i\xi_y$, v is the Poisson's ratio, G is the shear modulus of elasticity, $\kappa = 3 - 4v$ and $\kappa = (3 - v)/(1 + v)$ are the plane strain and stress problems respectively. A conjugated value is described by the bar over a function. By differentiating Equation (3) with respect to ξ as

$$\begin{aligned} N + iT &= \frac{d}{d\xi}(-Y + iX) \\ &= \phi'(\xi) + \overline{\phi'(\xi)} + \frac{d\bar{\xi}}{d\xi}(\xi\overline{\phi''(\xi)} + \overline{\psi'(\xi)}), \end{aligned} \tag{5}$$

the derivative in a specified direction (DISD) can be defined. The known normal and tangential tractions are represented by N and T respectively.

For the problem of cracks in a half-plane elasticity associated with the condition of traction free at the boundary of half-plane, the modified complex potentials (MCP) is applied. MCP constitutes of the principal and complementary parts describe as

$$\phi(\xi) = \phi_p(\xi) + \phi_c(\xi), \tag{6}$$
$$\phi'(\xi) = \phi'_p(\xi) + \phi'_c(\xi), \tag{7}$$
$$\psi(\xi) = \psi_p(\xi) + \psi_c(\xi), \tag{8}$$
$$\psi'(\xi) = \psi'_p(\xi) + \psi'_c(\xi), \tag{9}$$

where $\phi_p(\xi)$, $\phi'_p(\xi)$, $\psi_p(\xi)$, $\psi'_p(\xi)$ and $\phi_c(\xi)$, $\phi'_c(\xi)$, $\psi_c(\xi)$, $\psi'_c(\xi)$ represented the principal and complementary parts respectively. The principal part is attained from the crack opening displacements (COD) distribution along the crack faces in a problem of an infinite plate. The complex potentials of the principal part can be defined as

$$\phi_p(\xi) = \frac{1}{2\pi}\int_L \frac{g(\mu)d\mu}{\mu - \xi}, \tag{10}$$
$$\phi'_p(\xi) = \frac{1}{2\pi}\int_L \frac{g(\mu)d\mu}{(\mu - \xi)^2}, \tag{11}$$
$$\psi_p(\xi) = \frac{1}{2\pi}\int_L \frac{\overline{g(\mu)}d\mu}{\mu - \xi} + \frac{1}{2\pi}\int_L g(\mu)\left(\frac{d\bar{\mu}}{\mu - \xi} - \frac{\bar{\mu}d\mu}{(\mu - \xi)^2}\right), \tag{12}$$
$$\psi'_p(\xi) = \frac{1}{2\pi}\int_L \frac{\overline{g(\mu)}d\mu}{(\mu - \xi)^2} + \frac{1}{2\pi}\int_L g(\mu)\left(\frac{d\bar{\mu}}{(\mu - \xi)^2} - \frac{2\bar{\mu}d\mu}{(\mu - \xi)^3}\right). \tag{13}$$

COD is the unknown function which signifies by the $g(\mu)$ and is interpreted by

$$g(\mu) = \frac{2G}{i(\kappa + 1)}\Big[(u(\mu) + iv(\mu))^+ - (u(\mu) + iv(\mu))^-\Big], \quad \mu \in L. \tag{14}$$

The displacements at a point μ of the upper and lower parts of crack faces denote by $(u(\mu) + iv(\mu))^+$ and $(u(\mu)+iv(\mu))^-$ respectively. The traction at the boundary of half-plane caused by the principal part is eliminated by the complementary part. The condition of traction free along the boundary of half-plane (L_b), can be expressed by letting Equation (3) equal to zero as

$$\phi(\xi) + \xi\overline{\phi'(\xi)} + \overline{\psi(\xi)} = 0, \quad \xi \in L_b. \tag{15}$$

Next, using Equations (6) - (8), the condition (15) along the boundary of half-plane is written as

$$\Big[\overline{\phi_p(\xi)} + \overline{\phi_c(\xi)}\Big] + \xi\Big[\phi'_p(\xi) + \phi'_c(\xi)\Big] + \Big[\overline{\psi}_p(\xi) + \psi_c(\xi)\Big] = 0, \quad \xi \in L_b. \tag{16}$$

Then, substituting Equations (10) - (13) into Equation (16), after some manipulation, gives

$$\phi_c(\xi) = -\bar{\psi}_p(\xi) - \xi\bar{\phi}'_p(\xi), \tag{17}$$

$$\phi'_c(\xi) = -\bar{\phi}'_p(\xi) - \bar{\psi}'_p(\xi) - \xi\bar{\phi}''_p(\xi), \tag{18}$$

$$\psi_c(\xi) = -\bar{\phi}_p(\xi) + \xi\bar{\phi}'_p(\xi) + \xi\bar{\psi}'_p(\xi) + \xi^2\bar{\phi}''_p(\xi), \tag{19}$$

where $\bar{\phi}'_p(\xi)$ is an analytic function described by $\bar{\phi}'_p(\xi) = \overline{\phi'(\bar{\xi})}$. One obtains $\phi_c(\xi)$ and $\psi_c(\xi)$ from the established complex potentials $\phi_p(\xi)$ and $\psi_p(\xi)$. Hence, from (6) and (8), $\phi(\xi)$ and $\psi(\xi)$ are determined.

The crack problem in a half-plane is fomulated by applying the HSIE and represented by $[N(\mu_0) + iT(\mu_0)]_p$ and $[N(\mu_0) + iT(\mu_0)]_c$ which are the principal and complementary parts respectively. Substituting Equations (10) - (13) into Equation (5) to obtain the $[N(\mu_0) + iT(\mu_0)]_p$. Meanwhile, for the $[N(\mu_0)+iT(\mu_0)]_c$, we need to substitute Equations (17) - (19) into Equation (5). Then, letting ξ approach μ_0 and changing $d\bar{\xi}/d\xi$ by $d\bar{\mu}/d\mu$. By taking the observation point μ_0 on the crack L, the tractions are attained. Summing both parts $[N(\mu_0)+iT(\mu_0)]_p$ and $[N(\mu_0)+iT(\mu_0)]_c$ gives the following equations of a single crack problem [4]

$$\begin{aligned}[N(\mu_0) + iT(\mu_0)] =& \frac{1}{\pi} ⨎_L \frac{g(\mu)d\mu}{(\mu-\mu_0)^2} + \frac{1}{2\pi}\int_L \zeta_1(\mu,\mu_0)g(\mu)d\mu \\ &+ \frac{1}{2\pi}\int_L \zeta_2(\mu,\mu_0)\overline{g(\mu)}d\mu, \quad \mu_0 \in L\end{aligned} \tag{20}$$

where the kernals, ζ_1 and ζ_2 are described as

$$\begin{aligned}\zeta_1(\mu,\mu_0) =& -\frac{1}{(\mu-\bar{\mu}_0)^2} - \frac{2(\bar{\mu}_0-\bar{\mu})}{(\mu-\bar{\mu}_0)^3} - \frac{1}{(\mu-\mu_0)^2} - \frac{1}{(\mu-\bar{\mu}_0)^2}\frac{d\bar{\mu}}{d\mu} - \frac{1}{(\bar{\mu}-\mu_0)^2}\frac{d\bar{\mu}}{d\mu} \\ &+ \frac{d\bar{\mu}_0}{d\mu_0}\left(\frac{1}{(\mu-\bar{\mu}_0)^2}\frac{d\bar{\mu}}{d\mu} + \frac{1}{(\bar{\mu}-\bar{\mu}_0)^2}\frac{d\bar{\mu}}{d\mu} + \frac{2(\bar{\mu}_0-\mu_0)}{(\mu-\bar{\mu}_0)^3}\frac{d\bar{\mu}}{d\mu}\right. \\ &\left.+ \frac{6(\bar{\mu}_0-\bar{\mu})(\bar{\mu}_0-\mu_0)}{(\mu-\bar{\mu}_0)^4} + \frac{2(3\bar{\mu}_0-2\mu_0-\bar{\mu})}{(\mu-\bar{\mu}_0)^3}\right)\end{aligned}$$

$$\begin{aligned}\zeta_2(\mu,\mu_0) =& -\frac{1}{(\bar{\mu}-\mu_0)^2}\frac{d\bar{\mu}}{d\mu} - \frac{1}{(\bar{\mu}-\mu_0)^2} - \frac{1}{(\mu-\bar{\mu}_0)^2} + \frac{2(\mu-\mu_0)}{(\bar{\mu}-\mu_0)^3}\frac{d\bar{\mu}}{d\mu} + \frac{1}{(\bar{\mu}-\bar{\mu}_0)^2}\frac{d\bar{\mu}}{d\mu}, \\ &+ \frac{d\bar{\mu}_0}{d\mu_0}\left(\frac{1}{(\mu-\bar{\mu}_0)^2} + \frac{1}{(\bar{\mu}-\bar{\mu}_0)^2} + \frac{2(\mu_0-\mu)}{(\bar{\mu}-\bar{\mu}_0)^3}\frac{d\bar{\mu}}{d\mu} + \frac{2(\bar{\mu}_0-\mu_0)}{(\mu-\bar{\mu}_0)^3}\right).\end{aligned}$$

Let $N_j(\mu_{j0})+iT_j(\mu_{j0})$ denote the tractions applied at the point μ_{j0} of the crack-j and $j=1,2,3$ for the triple cracks problems. By superposition of the COD distribution $g_j(\mu_j)$ along the crack-j, HSIE of the triple cracks problem is attained as follows

$$\begin{aligned}N_j(\mu_{j0})+iT_j(\mu_{j0}) =& \frac{1}{\pi}⨎_L \frac{g_j(\mu_j)d\mu_j}{(\mu_j-\mu_{j0})^2} + \frac{1}{2\pi}\int_{L_j}\zeta_1(\mu_j,\mu_{j0})g_j(\mu_j)d\mu_j + \frac{1}{2\pi}\int_{L_j}\zeta_2(\mu_j,\mu_{j0})\overline{g_j(\mu_j)}d\mu_j \\ &+ \sum_{k=1}^{3}\left\{\frac{1}{\pi}\int_{L_k}\frac{g_k(\mu_k)d\mu_k}{(\mu_k-\mu_{j0})^2} + \frac{1}{2\pi}\int_{L_k}\zeta_1(\mu_k,\mu_{j0})g_k(\mu_k)d\mu_k\right. \\ &\left.+ \frac{1}{2\pi}\int_{L_k}\zeta_2(\mu_k,\mu_{j0})\overline{g_k(\mu_k)}d\mu_k\right\} + \sum_{m=1}^{3}\left\{\frac{1}{\pi}\int_{L_m}\frac{g_m(\mu_m)d\mu_m}{(\mu_m-\mu_{j0})^2}\right. \\ &\left.+ \frac{1}{2\pi}\int_{L_m}\zeta_1(\mu_m,\mu_{j0})g_m(\mu_m)d\mu_m + \frac{1}{2\pi}\int_{L_m}\zeta_2(\mu_m,\mu_{j0})\overline{g_m(\mu_m)}d\mu_m\right\}, \quad \mu_{j0}\in L_j\end{aligned} \tag{21}$$

where $j \neq k \neq m$.

The equal sign of the first integral signifies the hypersingular integral. Whereas the remaining integrals are defined as the regular integrals. The effect on crack-j influenced by itself is represented by the first three integrals, while the other integrals explain the effect of crack-k and crack-m on crack-j for $j = 1, 2, 3$ where $j \neq k \neq m$. Similar formulation can be found in [11].

Then, rewrite the solution (21) in the form of [2]

$$g_j(\mu_j)|_{\mu_j=\mu_j(s_j)} = \sqrt{a^2 - s_j^2} H_j(s_j) \quad \text{where} \quad H_j(s_j) = H_{j1}(s_j) + iH_{j2}(s_j) \tag{22}$$

for $j = 1, 2, 3$.

3 Numerical Examples

The stress intensity factor (SIF) at D_{jk} of crack-j for $j = 1, 2, 3$ and crack tips-k for $k = 1, 2$ are explained as follows

$$K_{D_{jk}} = (K_1 - iK_2)_{D_{jk}} = \sqrt{2\pi} \lim_{\mu \to \mu_{D_{jk}}} \sqrt{|\mu - \mu_{D_{jk}}|} g_j'(\mu_j) = \sqrt{\pi a_{jk}} F_{D_{jk}}, \tag{23}$$

where $F_{D_{jk}} = (F_{1D_{jk}} + iF_{2D_{jk}})$. $F_{1D_{jk}}$ and $F_{2D_{jk}}$ are Mode I and II of nondimensional SIFs at tips k of crack D_j.

Table 1: The nondimensional SIF of a circular arc crack with different opening angle, α, under shear loading $\sigma_x = p$.

SIF	α			
	10°	**20°**	**30°**	**40°**
F_{1A}*	0.9740	0.9009	0.7942	0.6712
F_{1A}**	0.9717	0.8977	0.7818	0.6312
F_{2A}*	0.1723	0.3319	0.4675	0.5708
F_{2A}**	0.1720	0.3318	0.4686	0.5714
F_{1B}*	0.9739	0.9008	0.7943	0.6712
F_{2B}*	-0.1723	-0.3318	-0.4675	-0.5708

*Current study
**[18]

Table 1 displays the behaviour of nondimensional SIFs F_1 and F_2 of a circular arc crack with opening angle, α, under shear loading $\sigma_x = p$. It is shown that F_1 at the tip of crack A is equal to F_1 at the tip of crack B. Meanwhile F_2 at the tip of crack A is equal to negative F_2 at the tip of crack B. From the table, we can analyse that at crack tip A, the values of F_1 decreases but F_2 increases as the crack opening angle increases. Our result is in good agreement with those of [18].

3.1 Example 1

Consider three adjacent circular arc cracks with opening angle α_1, α_2 and α_3 in a half-plane under shear loading and free traction boundary condition as presented in Figures 1(a) and 1(b).

The space between cracks is described by d and h is the distance between cracks and the boundary of half-plane. R_1, R_2 and R_3 are the radii of circular arc cracks respectively.

Figure 1(a) shows nondimensional SIFs F_1 and F_2 at all cracks tips for $h/R = 0.2$ and $\alpha = \alpha_1 = \alpha_2 = \alpha_3$ varies. As α varies, F_1 at A_1 is equal to F_1 at C_2 and F_1 at A_2 is equal to F_1 at C_1. It is found that B_1 and B_2 have the same value of F_1 as α increases. When $\alpha > 20°$, F_2 at A_1, B_1 and C_1 increases opposite to the behaviour of F_2 at A_2, B_2 and C_2. Whereas F_2 at A_2, B_2 and C_2 increases when $\alpha > 60°$.

Figure 1(b) represents the behaviour of F_1 and F_2 at all cracks tips for $\alpha = \alpha_1 = \alpha_2 = \alpha_3$ varies and $h/R = 0.2$. As $\alpha = \alpha_1 = \alpha_2 = \alpha_3$ increases, F_1 at all cracks tips decreases. F_1 at A_1 is equal to F_1 at C_2, F_1 at A_2 is equal to F_1 at C_1 and F_1 at B_1 is equal to F_1 at B_2 as h/R varies. When $\alpha > 60°$, at A_2, B_2 and C_2, F_2 increases opposite to the behaviour of F_2 at A_1, B_1 and C_1.

Figures 1(c) and 1(d) portray the nondimensional SIFs F_1 and F_2 for h/R varies and $\alpha = \alpha_1 = \alpha_2 = \alpha_3 = 45°$ for the cracks problem in Figure 1(b). As h/R varies, F_1 at A_1 is equal to F_1 at C_2, F_1 at A_2 is equal to F_1 at C_1 and F_1 at B_1 is equal to F_1 at B_2 (Figure 1(c)). Meanwhile F_1 at B_2 sharply decreases when $h/R > 2.5$ (Figure 1(c)). As h/R varies, F_2 do not show any significant difference at all cracks tips (Figure 1(d)). Whereas, when $h/R > 3.0$, F_2 at A_1, C_1 and B_2 slightly decreases (Figure 1(d)).

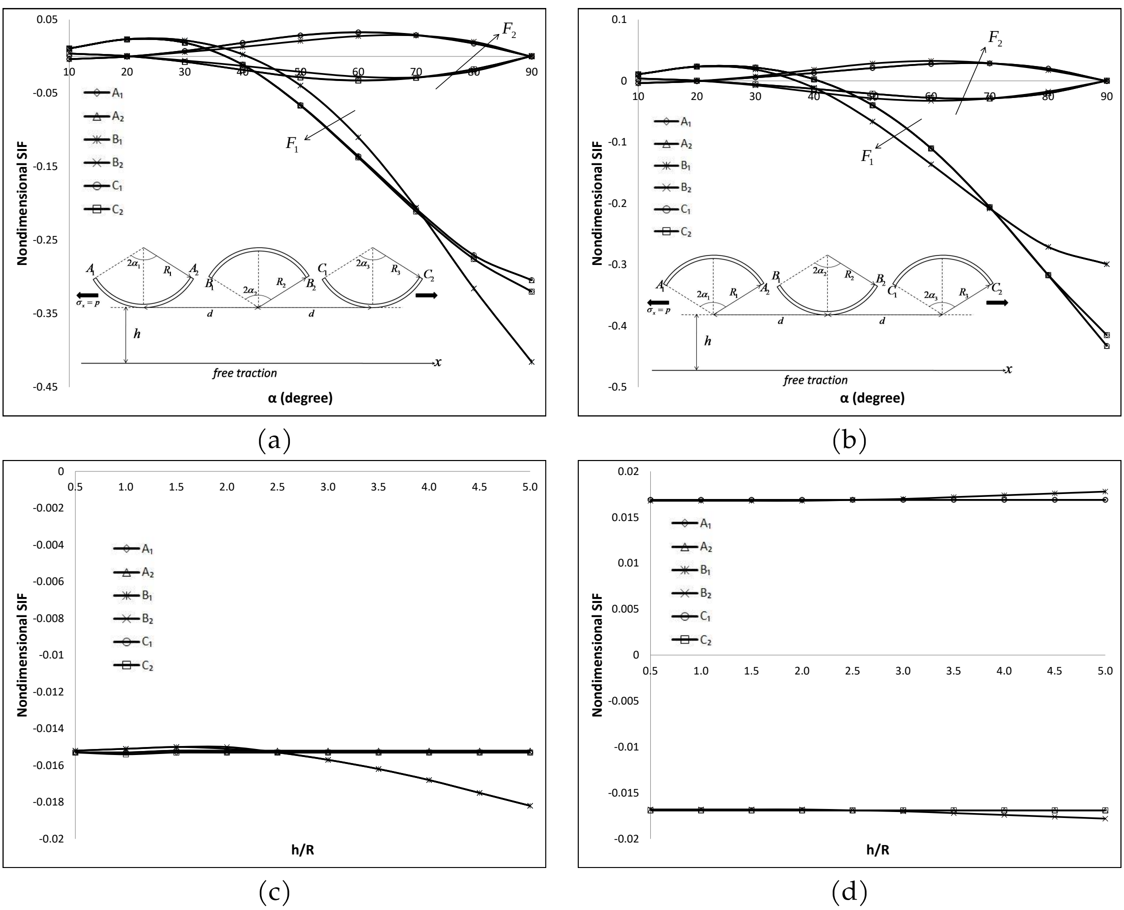

Figure 1: Three adjacent circular arc cracks in a half-plane: (a) and (b) the nondimensional SIFs when $\alpha = \alpha_1 = \alpha_2 = \alpha_3$ varies and $h/R = 0.2$; (c) F_1 and (d) F_2 for h/R varies and $\alpha = \alpha_1 = \alpha_2 = \alpha_3 = 45°$.

3.2 Example 2

Consider three circular arc cracks with opening angle α and dissimilar radius in a half-plane subjected to shear stress and free traction boundary condition as shown in Figures 2(a) and 2(c). R_1, R_2 and R_3 are denoted as radii of circular arc cracks respectively. h is the distance of cracks to the boundary of half-plane and the space between each crack is defined by d.

Figures 2(a) and 2(b) display the behaviour of F_1 and F_2 at all cracks tips as α varies and $h/R = 0.1$ for the problem of cracks in Figure 2(a). As α increases, F_1 at A_1 is equal to F_1 at A_2, F_1 at B_1 is equal to F_1 at B_2 and F_1 at C_1 is equal to F_1 at C_2 (Figure 2(a)). When $\alpha > 20°$, F_2 at A_1 is equal to negative F_2 at A_2 and F_2 at C_1 is equal to negative F_2 at C_2 (Figure 2(b)). Whereas F_2 at B_2 increase sharply opposite to the behaviour of F_2 at B_1 when $\alpha > 40°$ (Figure 2(b)).

Figures 2(c) and 2(d) represent the nondimensional SIFs F_1 and F_2 when $h/R = 0.1$ and α varies for the cracks problem in Figure 2(c). F_1 at B_1 and B_2 increases as α increases (Figure 2(c)). When $\alpha > 70°$, F_2 at B_2 has the highest value of SIF opposite to the behaviour of F_2 at B_1 (Figure 2(d)).

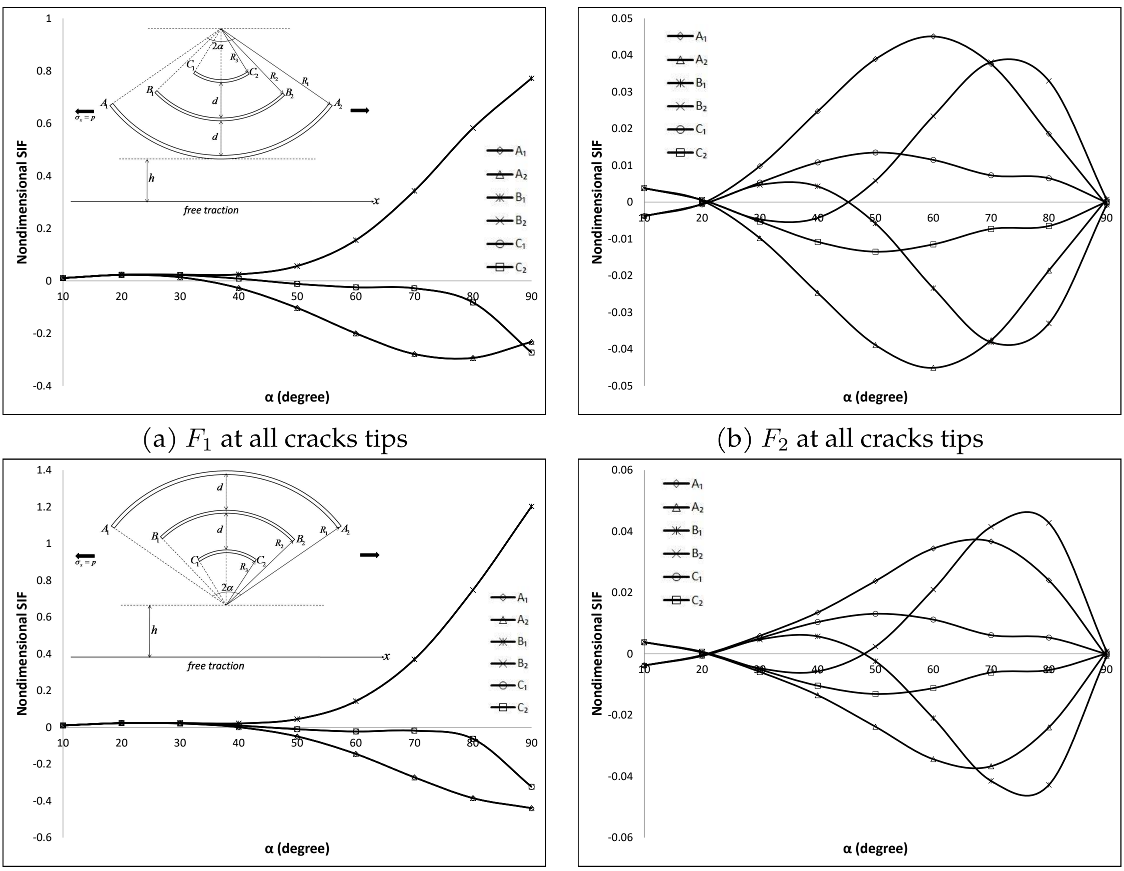

(a) F_1 at all cracks tips

(b) F_2 at all cracks tips

(c) F_1 at all cracks tips

(d) F_2 at all cracks tips

Figure 2: Three circular arc cracks problem with dissimilar radius in a half-plane: (a), (b), (c) and (d) the nondimensional SIFs when α varies and $h/R = 0.1$.

3.3 Example 3

Consider three circular arc cracks in series with opening angle α_1, α_2 and α_3 in a half-plane subjected to shear stress and free traction boundary condition as shown in Figures 3(a) and 3(b). R_1, R_2 and R_3 are defined as radii of circular arc cracks respectively. The space between cracks is d and h is the distance of cracks to the boundary of half-plane.

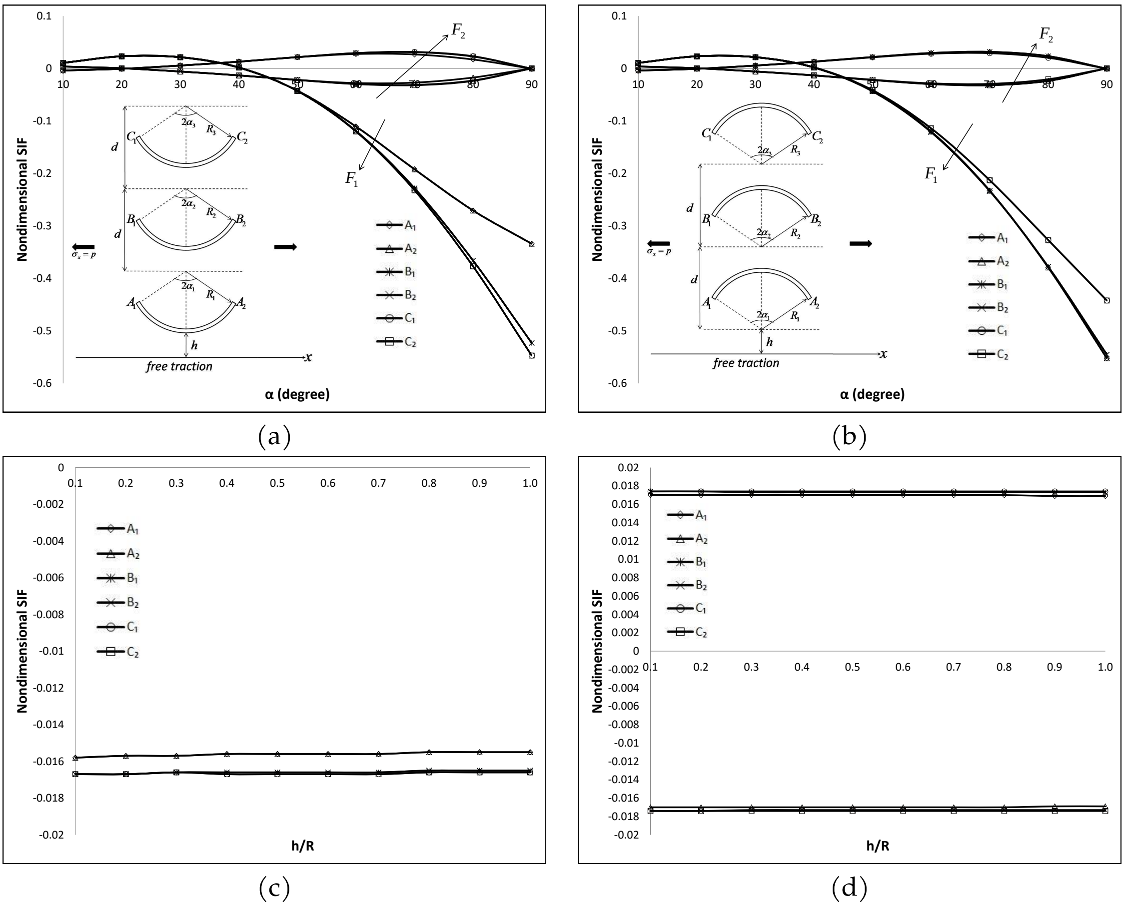

Figure 3: Three circular arc cracks in series in a half-plane: (a) and (b) the nondimensional SIFs when $\alpha = \alpha_1 = \alpha_2 = \alpha_3$ varies and $h/R = 0.5$; (c) F_1 and (d) F_2 for h/R varies and $\alpha = \alpha_1 = \alpha_2 = \alpha_3 = 45°$.

Figure 3(a) portrays the nondimensional SIFs for both F_1 and F_2 at all cracks tips as $\alpha = \alpha_1 = \alpha_2 = \alpha_3$ varies and $h/R = 0.5$. It is found that F_1 at A_1 is equal to F_1 at A_2, F_1 at B_1 is equal to F_1 at B_2 and F_1 at C_1 is equal to F_1 at C_2 as α increases. F_1 decreases as α increases at all cracs tips. When $\alpha > 20°$, F_2 at A_1, B_1 and C_1 increases but F_2 at A_2, B_2 and C_2 decreases. Whereas F_2 at A_1, B_1 and C_1 decreases when $\alpha > 70°$ opposite to the behaviour of F_2 at A_2, B_2 and C_2.

Figure 3(b) displays the nondimensional SIFs F_1 and F_2 for $h/R = 0.5$ and $\alpha = \alpha_1 = \alpha_2 = \alpha_3$ varies. As α increases, F_1 at all cracks tips decreases. It is observed that F_2 at A_1, B_1 and C_1 increases but F_2 at A_2, B_2 and C_2 decreases when $\alpha > 20°$. Meanwhile when $\alpha > 70°$, F_2 at A_2, B_2 and C_2 increases opposite to the behaviour of F_2 at A_1, B_1 and C_1.

Figures 3(c) and 3(d) show the nondimensional SIFs F_1 and F_2 when h/R varies and $\alpha =$

$\alpha_1 = \alpha_2 = \alpha_3 = 45°$ for the cracks problem in Figure 3(a). F_1 at all cracks tips remains constant as h/R increases (Figure 3(c)). As h/R increases, F_2 at A_1 is equal to negative F_2 at A_2, F_2 at B_1 is equal to negative F_2 at B_2 and F_2 at C_1 is equal to negative F_2 at C_2 (Figure 3(d)).

4 Conclusions

In this paper, three circular arc cracks problem subjected to shear loading in a half-plane elasticity is considered. By applying the free traction boundary condition, the problem is formulated into HSIE associated with the modified complex potentials. Appropriate quadrature formulas is utilised to solve the equations numerically. From the results, we can analyse that the behaviour of nondimensional SIFs for both Mode I and II at all cracks tips is influenced by the crack opening angle of circular arc cracks and the distance between cracks to the boundary of half-plane. As the angle increases and the distance of cracks closer to the boundary of half-plane, SIF increases. The strength of material decreases as SIF increases.

Acknowledgement The author would like to thank Ministry of Higher Education for the Fundamental Research Grant Scheme, Project No: FRGS/1/2019/STG06/UPM/02/5 Vot No. 9567900.

Conflicts of Interest The authors declare no conflict of interest.

References

[1] N. Akhtar & S. Hasan (2017). Assessment of the interaction between three collinear unequal straight cracks with unified yield zones. *AIMS Materials Science*, *4*(2), 302–316.

[2] Y. Z. Chen (2004). Solution of integral equation in curve crack problem by using curve length coordinate. *Engineering Analysis with Boundary Elements*, *28*(8), 989–994.

[3] Y. Z. Chen & Y. K. Cheung (1990). New integral equation approach for the crack problem in elastic half-plane. *International Journal of Fracture*, *46*(1), 57–69.

[4] Y. Z. Chen, X. Y. Lin & X. Z. Wang (2009). Numerical solution for curved crack problem in elastic half-plane using hypersingular integral equation. *Philosophical Magazine*, *89*(26), 2239–2253.

[5] S. Das & L. Debnath (2003). Interaction between griffith cracks in a sandwiched orthotropic layer. *Applied Mathematics Letters*, *16*(4), 609–617.

[6] S. Das, B. Patra & L. Debnath (2001). Interaction between three moving griffith cracks at the interface of two dissimilar elastic media. *Korean Journal of Computational & Applied Mathematics*, *8*(1), 59–69.

[7] N. R. F. Elfakhakhre, N. M. A. Nik Long & Z. K. Eshkuvatov (2018). Stress intensity factor for an elastic half plane weakened by multiple curved cracks. *Applied Mathematical Modelling*, *60*, 540–551.

[8] N. R. F. Elfakhakhre, N. M. A. Nik Long & Z. K. Eshkuvatov (2019). Numerical solutions for cracks in an elastic half-plane. *Acta Mechanica Sinica*, *35*(1), 212–227.

[9] N. Hallback & M. W. Tofique (2014). Development of a distributed dislocation dipole technique for the analysis of multiple straight, kinked and branched cracks in an elastic half-plane. *International Journal of Solids and Structures*, *51*(15-16), 2878–2892.

[10] Z. Y. Huang, R. H. Bao & Z. G. Bian (2007). The potential theory method for a half-plane crack and contact problems of piezoelectric materials. *Composite Structures*, *78*(4), 596–601.

[11] N. H. Husin, N. M. A. Nik long & N. Senu (2019). Hypersingular integral equation for triple inclined cracks problems in half plane elasticity. In *Journal of Physics: Conference Series*, pp. 012023. IOP Publishing, Kuantan, Pahang. https://doi.org/10.1088/1742-6596/1366/1/012023.

[12] S. Itou (2013). Stress intensity factors for three cracks at the interfaces of a graded layer bonding two different materials. *Applied Mathematical Modelling*, *37*(4), 2516–2530.

[13] S. Itou (2016). Dynamic stress intensity factors of three collinear cracks in an orthotropic plate subjected to time-harmonic disturbance. *Journal of Mechanics*, *32*(5), 491–499.

[14] M. M. Monfared & M. Ayatollahi (2015). Cracking in orthotropic half-plane with a functionally graded coating under anti-plane loading. *Acta Mechanica Solida Sinica*, *28*(2), 210–220.

[15] M. M. Monfared, M. Ayatollahi & S. M. Mousavi (2016). The mixed-mode analysis of a functionally graded orthotropic half-plane weakened by multiple curved cracks. *Archive of Applied Mechanics*, *86*(4), 713–728.

[16] N. I. Muskhelishvili (1953). *Some basic problems of the mathematical theory of elasticity*. Springer, Dordrecht, Eastern Cape.

[17] T. Sadowski, E. M. Craciun, A. Rabaea & L. Marsavina (2016). Mathematical modeling of three equal collinear cracks in an orthotropic solid. *Meccanica*, *51*(2), 329–339.

[18] X. Yan (2010). A boundary element analysis for stress intensity factors of multiple circular arc cracks in a plane elasticity plate. *Applied Mathematical Modelling*, *34*(10), 2722–2737.